

Supplement of Hydrol. Earth Syst. Sci., 24, 2791–2815, 2020
<https://doi.org/10.5194/hess-24-2791-2020-supplement>
© Author(s) 2020. This work is distributed under
the Creative Commons Attribution 4.0 License.



Supplement of

Modelling rainfall with a Bartlett–Lewis process: new developments

Christian Onof and Li-Pen Wang

Correspondence to: Christian Onof (c.onof@imperial.ac.uk)

The copyright of individual parts of the supplement might differ from the CC BY 4.0 License.

S1 Relation between cell intensity parameters

In the model equations, parameters μ_x , f_1 and f_2 for the RBL1 and ι , f_1 and f_2 for the RBL2 are three unrelated model parameters only if a three-parameter distribution is chosen for the cell intensity. If a two-parameter distribution is chosen, there will effectively be two unrelated parameters, if a one-parameter distribution is chosen, there will only be one.

Starting with the last case first, the standard choice is the exponential distribution:

$$f_X(x) = ae^{-ax} \text{ for } x > 0$$

for which:

$$\mu_x = 1/a$$

$$f_1 = 2$$

$$f_2 = 6$$

So, for the exponential distribution, the only free parameter is μ_x for the RBL1 and ι for the RBL2.

Next, we can seek to have more flexibility by using the Gamma distribution:

$$f_X(x) = \frac{x^{a-1}e^{-x/b}}{b^a\Gamma(a)} \text{ for } x > 0$$

for which:

$$\mu_x = ab$$

$$f_1 = \frac{a+1}{a}$$

$$f_2 = \frac{a^2+3a+2}{a^2}$$

So, for the Gamma distribution there would be two free parameters μ_x or ι , and f_1 , with f_2 obtained as the following function of f_1 :

$$f_2 = 2f_1^2 - f_1.$$

The Pareto distribution is a thick-tailed distribution that will produce larger extremes:

$$f_X(x) = \frac{ab^a}{x^{a+1}} \text{ for } x \geq b$$

and for the distribution, we have:

$$\mu_x = \frac{ab}{a-1} \text{ (if } a > 1)$$

$$f_1 = \frac{(a-1)^2}{a(a-2)} \text{ (if } a > 2 \text{ i.e. } f_1 > 1)$$

$$f_2 = \frac{(a-1)^3}{a^2(a-3)} \text{ (if } a > 3 \text{ i.e. } f_2 > 1)$$

For the Pareto distribution there would also be two free parameters μ_x or ι , and f_1 , with f_2 obtained as the following function of f_1 :

$$f_2 = \frac{f_1^{3/2}}{f_1^{1/2}(3-2f_1)-2(f_1-1)^{3/2}}$$

where we have to have $f_1 < 4/3$ to fulfil the condition $a > 3$.

Finally, a mixed distribution could be chosen, e.g. one which is a mixture of Gamma and Pareto, with weight ω representing the probability of sampling from a Gamma rather than a Pareto. This would be defined by the following pdf:

$$f_X(x) = \omega \frac{x^{a-1}e^{-x/b}}{b^a\Gamma(a)} + (1 - \omega) \frac{cd^c}{x^{c+1}} \text{ for } x \geq d$$

for which the moments are just weighted combinations of those of the Gamma and Pareto distributions:

$$\mu_x = \omega ab + (1 - \omega) \frac{cd}{c-1} \text{ (if } c > 1)$$

$$f_1 = \frac{\omega(a+1)ab^2 + (1-\omega)\frac{cd^2}{c-2}}{\left(\omega ab + (1-\omega)\frac{cd}{c-1}\right)^2} \text{ (if } c > 2)$$

$$f_2 = \frac{\omega(a^2+3a+2)ab^3 + (1-\omega)\frac{cd^3}{c-3}}{\left(\omega ab + (1-\omega)\frac{cd}{c-1}\right)^3} \text{ (if } c > 3)$$

Here, we would have three free parameters, μ_x , f_1 and f_2 and for the purposes of simulation, we would seek parameters ω , a , b , c and d for which the three right-hand sides of the above equations would be equal to μ_x , f_1 and f_2 , for instance by minimising a sum of squares. This optimisation problem is underdetermined, but it would make sense to choose at least for the Gamma parameters a and b values close to values obtained when fitting a Gamma distribution as starting values, or indeed to fix these two parameters to these values.

S2 Example of integral divergence

The integral of a sum of terms is only equal to the sum of the integrals of each additive term when the latter are finite. When the latter are infinite, this is not necessarily the case. That is, it is possible that the integral of the sum should be finite while the integrals of the additive terms are infinite. This section shows an example to illustrate this.

Consider the following integrals:

$$I(x) = \int_0^x \frac{e^{\omega t} - e^{-\sigma t}}{t} dt$$

$$I_1(x) = \int_0^x \frac{e^{\omega t}}{t} dt$$

$$I_2(x) = \int_0^x -\frac{e^{-\sigma t}}{t} dt$$

The integrals $I_1(x)$ and $I_2(x)$ are divergent integrals because the integrands behave as $1/t$ and $-1/t$ respectively, in the vicinity of zero. So $I_1(x) = +\infty$ and $I_2(x) = -\infty$.

However, using Taylor expansions, we can see that $I(x)$ is finite:

$$\begin{aligned} I(x) &= \int_0^x \frac{1 + \omega t - 1 + \sigma t + O(t)}{t} dt \\ &= \int_0^x \omega + \sigma + O(1) dt \end{aligned}$$

Therefore:

$$I(x) = (\omega + \sigma)x + O(x)$$

and

$$I(x) \neq I_1(x) + I_2(x)$$

S3 Proportion dry

S3.1 Theoretical constraint

Based upon the theoretical form of the proportion of dry periods (or proportion dry) given as in Rodriguez-Iturbe et al (1988) (see equation (2.5)) and taking expectations over the term which is exponentiated, one can obtain the following expression for the proportion dry (Onof and Wheater, 1993):

$$P_d(h) = \exp \left[-\lambda(h + \mu_T) + \frac{\lambda v e^{-\kappa}}{\alpha - 1} \times \frac{\phi + \kappa \left(\frac{v}{v + (\kappa + \phi)h} \right)^{\alpha-1}}{\phi + \kappa} \int_0^1 t^{\phi-1} (1-t) e^{\kappa t} dt \right]$$

This equation can be further approximated as follows:

$$P_d(h) \approx \exp \left[-\lambda(h + \hat{\mu}_{T_M}) + \frac{\lambda v e^{-\kappa}}{\alpha - 1} \times \frac{\phi + \kappa \left(\frac{v}{v + (\kappa + \phi)h} \right)^{\alpha-1}}{\phi + \kappa} \hat{I}_{M'} \right]$$

where $\hat{\mu}_{T_M}$ (the approximation of the mean storm duration, μ_T) and $\hat{I}_{M'}$ are computed using the following formulae:

$$\hat{\mu}_{T_M} = \frac{v}{\alpha - 1} \left(1 + \phi \sum_{j=1}^M \frac{(-\kappa)^{j-1} (\kappa - j^2 - j)}{j(j+1)!} B(j+1, \phi) + \phi^{-1} \right)$$

and

$$\hat{I}_{M'} = \sum_{j=0}^{M'} \frac{\kappa^j}{j!} B(j + \phi, 2) + \frac{\delta_{M'}(\kappa)}{(M' + \phi + 1)(M' + \phi + 2)}$$

with

$$\delta_{M'}(\kappa) = e^{\kappa} - \sum_{j=0}^{M'} \frac{\kappa^j}{j!}$$

where $B(\cdot)$ is Beta function, and M and M' are to be chosen large enough to obtain satisfactory approximation. For details about the derivations and an investigation into the magnitude of the errors incurred in using these approximations, see Wheater et al. (2006, equations (B.80) and (B.89)).

We note that the constraint for α is $\alpha > 1$. The constraint for α in the new RBL2-sM-NC model is however $\alpha > 0$, and, as summarised in Table 4 in the main paper, the obtained values of α are mostly smaller than or very close to 1. Therefore, the theoretical proportion dry can hardly be derived using the approximate equation given above.

S3.2 Sampling strategy

This issue can however be addressed through sampling. We had found that the underestimation of proportion dry is due to the generation of many tiny amounts of rainfall which are not significant for any hydrological application. If we therefore look rather at the proportion of near-dry periods (with rainfall below a small threshold of 0.01 mm per 5-min) the problem disappears at hourly and

sub-hourly scales. A comparison is given in Figure S1 of proportion dry statistics derived from 250 simulations of RBL2-sM-NC, RBL2-sM and RBL2-bM models, respectively. As can be seen, the new RBL2-sM-NC can better reproduce proportion dry statistics at 5-min and 1-h timescales than RBL2-sM and RBL2-bM models. However, the RBL2-bM model starts to outperform the other two models at supra-hourly timescales.

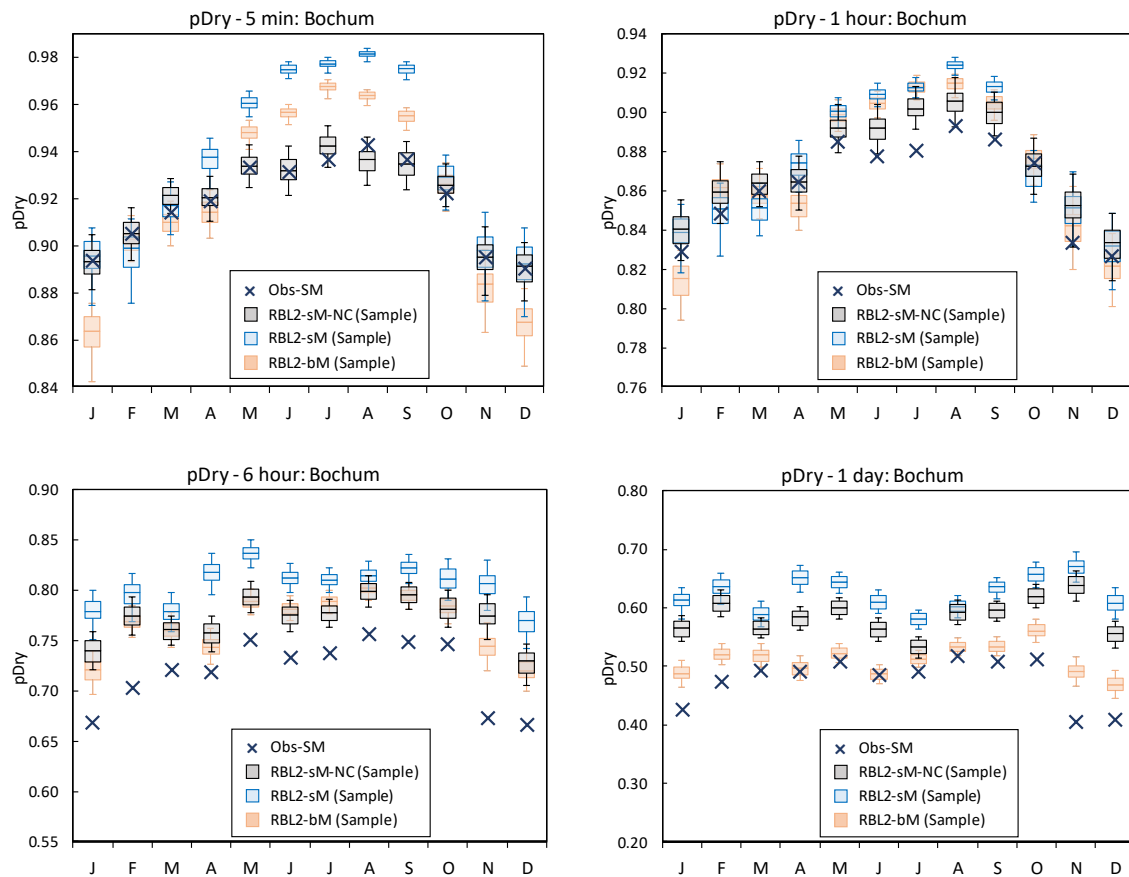


Fig. S1: Proportion dry (pDry) by month at Bochum: the observed (Obs-sM, cross markers), and the simulated ones sampled with RBL2-bM (light orange boxplots), RBL2-sM (light blue boxplots), and RBL2-sM-NC (black boxplots) models.

S4 Fitted parameters and simulation results obtained from Uccle rain gauge records

S4.1 Fitted parameters

Table S1: Parameters for RBL1-sM model using Uccle gauge data; constraint: $\alpha > 4$.

| Month | λ | μ_x | α | α/ν | κ | φ |
|-------|-----------|---------|----------|--------------|----------|-----------|
| Jan | 0.031 | 1.433 | 4.000 | 11.227 | 0.622 | 0.038 |
| Feb | 0.029 | 1.259 | 4.372 | 11.757 | 0.682 | 0.036 |
| Mar | 0.026 | 1.724 | 4.406 | 13.614 | 0.503 | 0.028 |
| Apr | 0.028 | 2.166 | 4.421 | 14.305 | 0.350 | 0.026 |
| May | 0.022 | 5.655 | 4.929 | 12.541 | 0.150 | 0.026 |
| Jun | 0.023 | 6.375 | 4.017 | 13.474 | 0.127 | 0.025 |
| Jul | 0.019 | 11.810 | 7.092 | 10.514 | 0.047 | 0.015 |
| Aug | 0.022 | 8.009 | 4.693 | 17.593 | 0.185 | 0.028 |
| Sep | 0.020 | 6.303 | 5.836 | 12.917 | 0.131 | 0.020 |
| Oct | 0.021 | 2.767 | 4.000 | 12.702 | 0.351 | 0.024 |
| Nov | 0.029 | 1.522 | 4.000 | 11.921 | 0.631 | 0.032 |
| Dec | 0.032 | 1.437 | 4.000 | 11.308 | 0.797 | 0.044 |

Table S2: Parameters for RBL1-sM-NC model using Uccle gauge data; constraint: $\alpha > 1$.

| Month | λ | μ_x | α | α/ν | κ | φ |
|-------|-----------|---------|----------|--------------|----------|-----------|
| Jan | 0.034 | 1.411 | 3.388 | 12.673 | 0.578 | 0.036 |
| Feb | 0.029 | 1.259 | 4.372 | 11.757 | 0.682 | 0.036 |
| Mar | 0.026 | 1.724 | 4.406 | 13.614 | 0.503 | 0.028 |
| Apr | 0.028 | 2.166 | 4.421 | 14.305 | 0.350 | 0.026 |
| May | 0.022 | 5.655 | 4.929 | 12.541 | 0.150 | 0.026 |
| Jun | 0.024 | 7.119 | 3.846 | 17.031 | 0.132 | 0.023 |
| Jul | 0.019 | 11.810 | 7.092 | 10.514 | 0.047 | 0.015 |
| Aug | 0.022 | 8.009 | 4.693 | 17.593 | 0.185 | 0.028 |
| Sep | 0.020 | 6.303 | 5.836 | 12.917 | 0.131 | 0.020 |
| Oct | 0.021 | 2.764 | 3.887 | 12.970 | 0.347 | 0.024 |
| Nov | 0.029 | 1.551 | 4.013 | 12.305 | 0.638 | 0.031 |
| Dec | 0.036 | 1.411 | 3.094 | 11.457 | 0.623 | 0.042 |

Table S3: Parameters for RBL2-sM model using Uccle gauge data; constraint: $\alpha > 2$.

| Month | λ | l | α | α/ν | κ | φ |
|-------|-----------|-------|----------|--------------|----------|-----------|
| Jan | 0.019 | 0.172 | 2.000 | 7.809 | 0.859 | 0.032 |
| Feb | 0.019 | 0.231 | 2.000 | 4.766 | 0.699 | 0.040 |
| Mar | 0.017 | 0.216 | 2.000 | 7.528 | 0.592 | 0.029 |
| Apr | 0.019 | 0.212 | 2.000 | 11.093 | 0.451 | 0.024 |
| May | 0.014 | 0.942 | 2.000 | 6.016 | 0.170 | 0.032 |
| Jun | 0.013 | 1.277 | 2.000 | 4.588 | 0.098 | 0.023 |
| Jul | 0.015 | 1.905 | 2.000 | 5.790 | 0.039 | 0.014 |
| Aug | 0.013 | 1.031 | 2.000 | 7.673 | 0.168 | 0.027 |
| Sep | 0.014 | 0.854 | 2.000 | 7.043 | 0.144 | 0.024 |
| Oct | 0.013 | 0.410 | 2.000 | 6.893 | 0.427 | 0.026 |
| Nov | 0.019 | 0.198 | 2.000 | 7.375 | 0.798 | 0.030 |
| Dec | 0.019 | 0.206 | 2.001 | 6.227 | 0.968 | 0.038 |

Table S4: Parameters for RBL2-sM-NC model using Uccle gauge data; constraint: $\alpha > 0$.

| Month | λ | l | α | α/ν | κ | φ |
|-------|-----------|-------|----------|--------------|----------|-----------|
| Jan | 0.018 | 0.167 | 0.892 | 7.043 | 0.876 | 0.030 |
| Feb | 0.019 | 0.142 | 1.175 | 7.731 | 0.891 | 0.031 |
| Mar | 0.017 | 0.181 | 1.040 | 8.387 | 0.650 | 0.026 |
| Apr | 0.018 | 0.266 | 1.026 | 7.444 | 0.414 | 0.026 |
| May | 0.014 | 0.718 | 0.542 | 5.831 | 0.331 | 0.045 |
| Jun | 0.011 | 0.980 | 0.502 | 5.585 | 0.211 | 0.028 |
| Jul | 0.016 | 1.874 | 0.595 | 4.546 | 0.072 | 0.029 |
| Aug | 0.012 | 0.867 | 0.682 | 8.448 | 0.214 | 0.025 |
| Sep | 0.015 | 0.807 | 0.560 | 5.960 | 0.210 | 0.034 |
| Oct | 0.013 | 0.425 | 0.865 | 5.514 | 0.431 | 0.027 |
| Nov | 0.018 | 0.183 | 1.125 | 7.446 | 0.837 | 0.028 |
| Dec | 0.018 | 0.094 | 0.789 | 13.487 | 1.157 | 0.020 |

S4.2 Simulation results

S4.2.1 Standard statistics

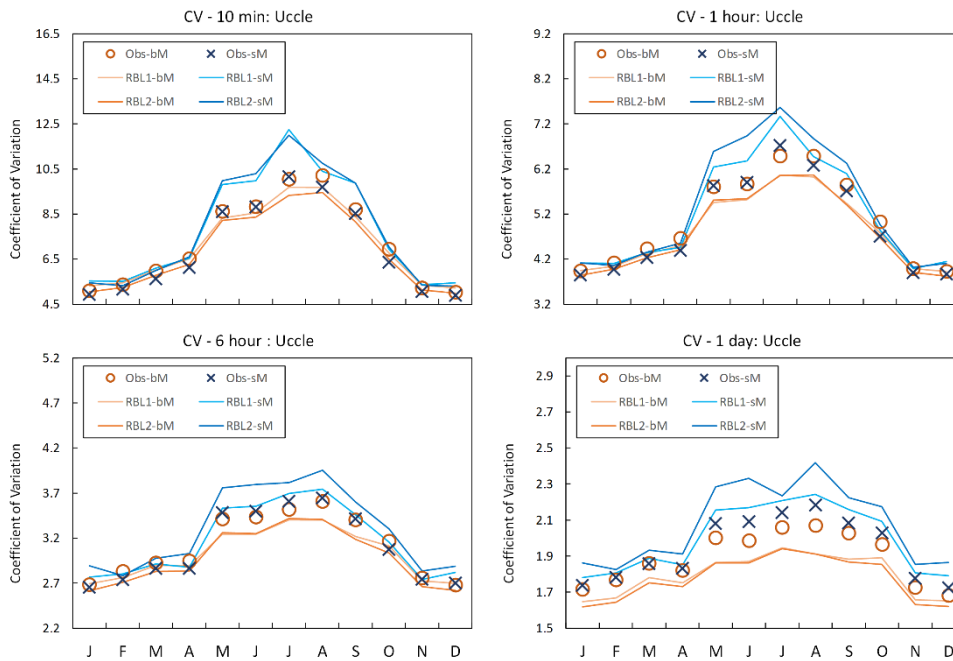


Fig. S2: Coefficient of variation (CV) by month at Uccle: the observed calculated with block (Obs-bM, orange circle markers) vs. standard (Obs-sM, blue cross markers) methods, the fitted one with RBL1 (RBL1-bM, light orange line; RBL1-sM, light blue line) models, and the fitted one with RBL2 (RBL2-bM, orange lines; RBL2-sM, blue lines) models.

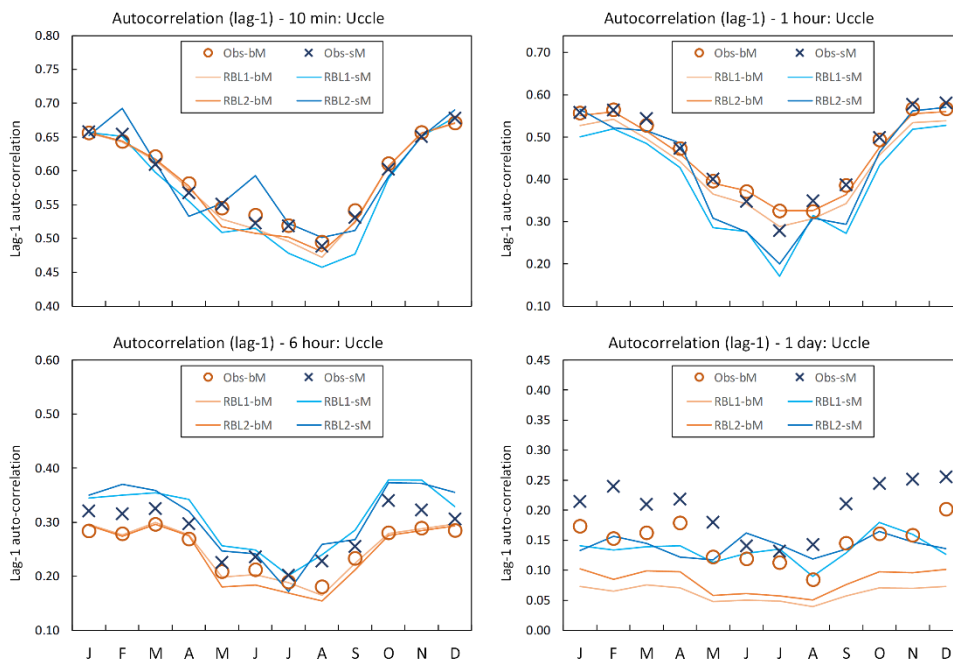


Fig. S3: Autocorrelation lag-1 by month at Uccle: the observed calculated with block (Obs-bM, orange circle markers) vs. standard (Obs-sM, blue cross markers) methods, the fitted one with RBL1 (RBL1-bM, light orange line; RBL1-sM, light blue line) models, and the fitted one with RBL2 (RBL2-bM, orange lines; RBL2-sM, blue lines) models.

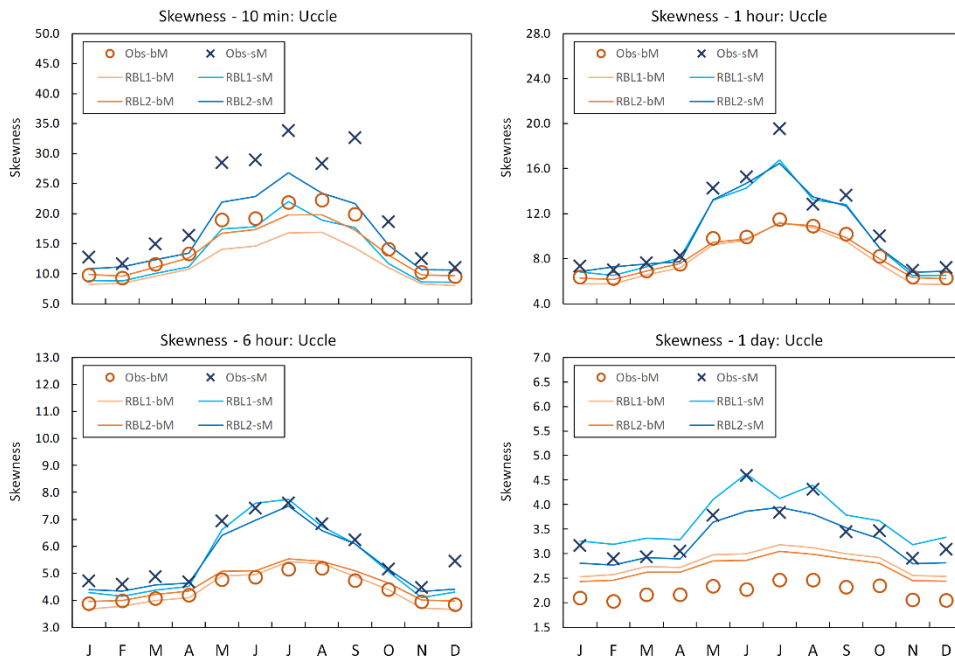


Fig. S4: Coefficient of skewness by month at Uccle: the observed calculated with block (Obs-bM, orange circle markers) vs. standard (Obs-sM, blue cross markers) methods, the fitted one with RBL1 (RBL1-bM, light orange line; RBL1-sM, light blue line) models, and the fitted one with RBL2 (RBL2-bM, orange lines; RBL2-sM, blue lines) models.

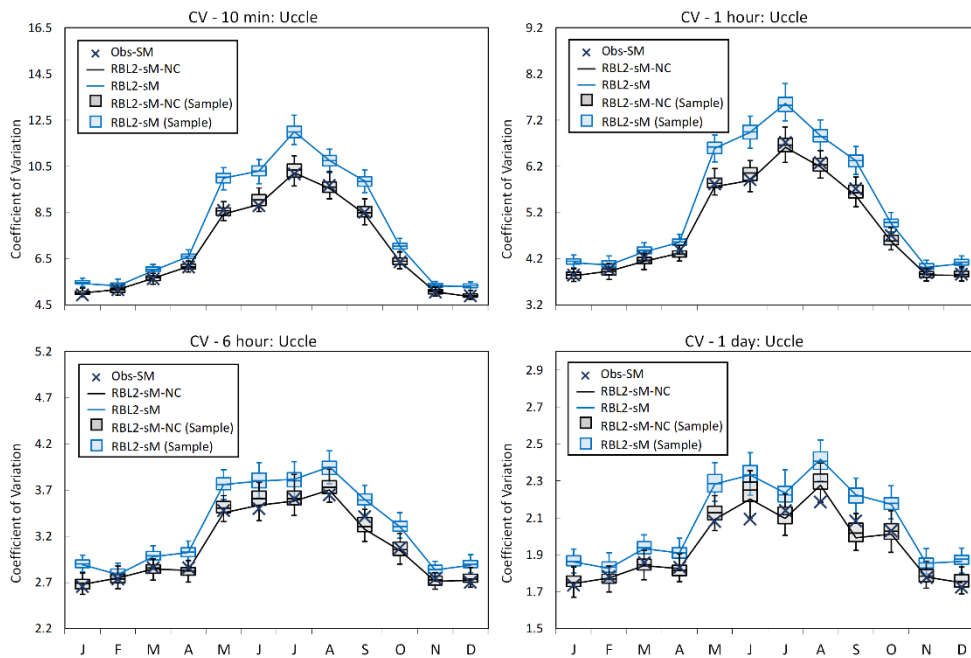


Fig. S5: Coefficient of variation (CV) by month at Uccle: the observed vs. the fitted one using RBL2 models with the original and the new extended parameter spaces for α (RBL2-sM, light blue lines and boxplots; RBL2-sM-NC, black lines and boxplots).

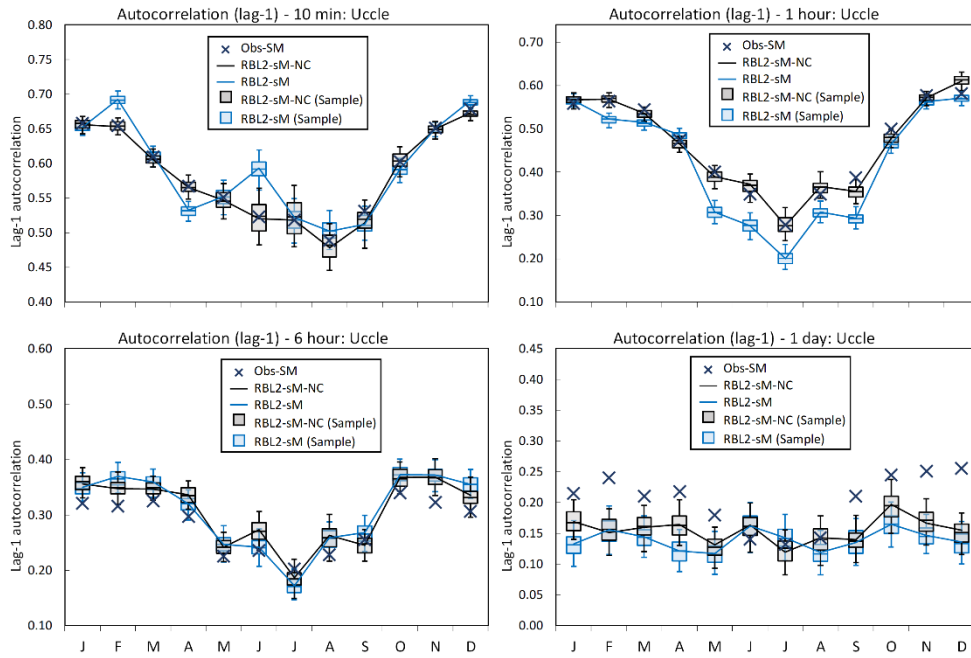


Fig. S6: Autocorrelation lag-1 by month at Uccle: the observed vs. the fitted one using RBL2 models with the original and the new extended parameter spaces for α (RBL2-sM, light blue lines and boxplots; RBL2-sM-NC, black lines and boxplots).

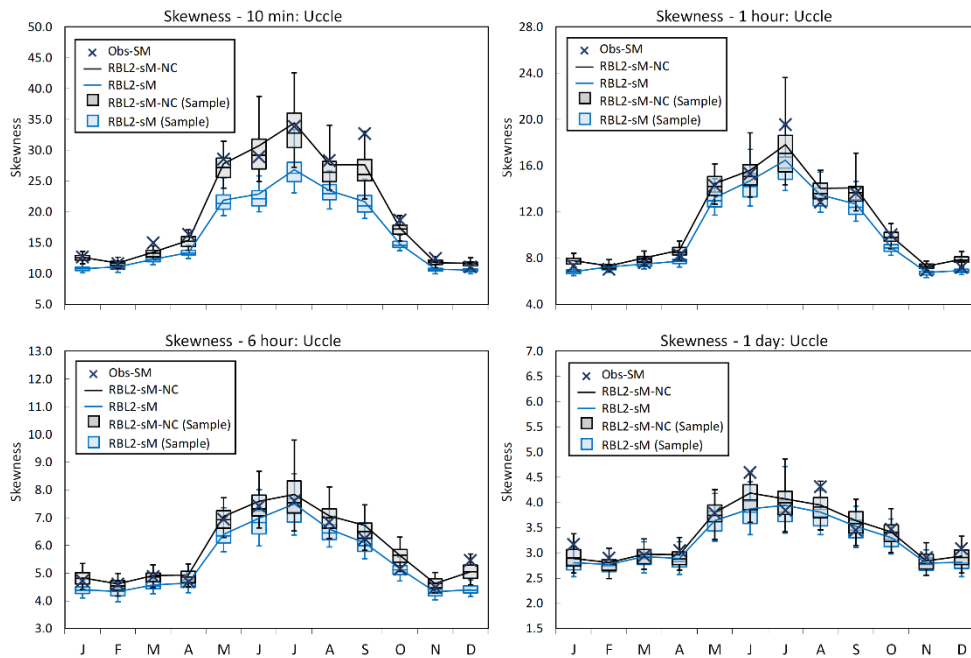


Fig. S7: Coefficient of skewness by month at Uccle: the observed vs. the fitted one using RBL2 models with the original and the new extended parameter spaces for α (RBL2-sM, light blue lines and boxplots; RBL2-sM-NC, black lines and boxplots).

S4.2.2 Extreme value statistics

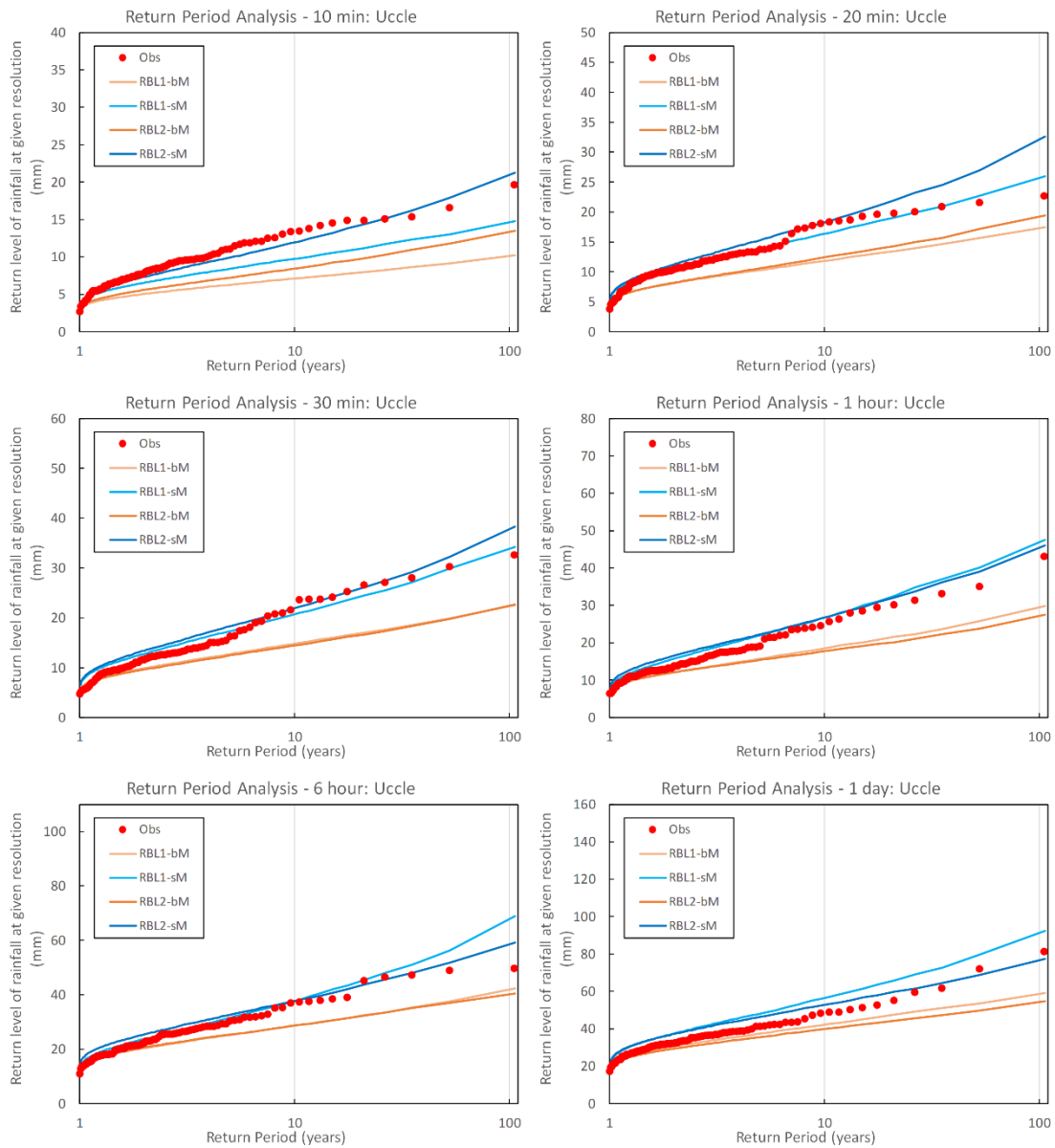


Fig. S8: Observed (round markers) and simulated (lines) return levels of rainfall at different timescales at Uccle. The simulated is sampled from the RBL1 and RBL2 models fitted with selected statistical properties calculated using bM and sM methods, respectively; and the median return levels obtained from 250 simulations, each of 105 years, are illustrated.

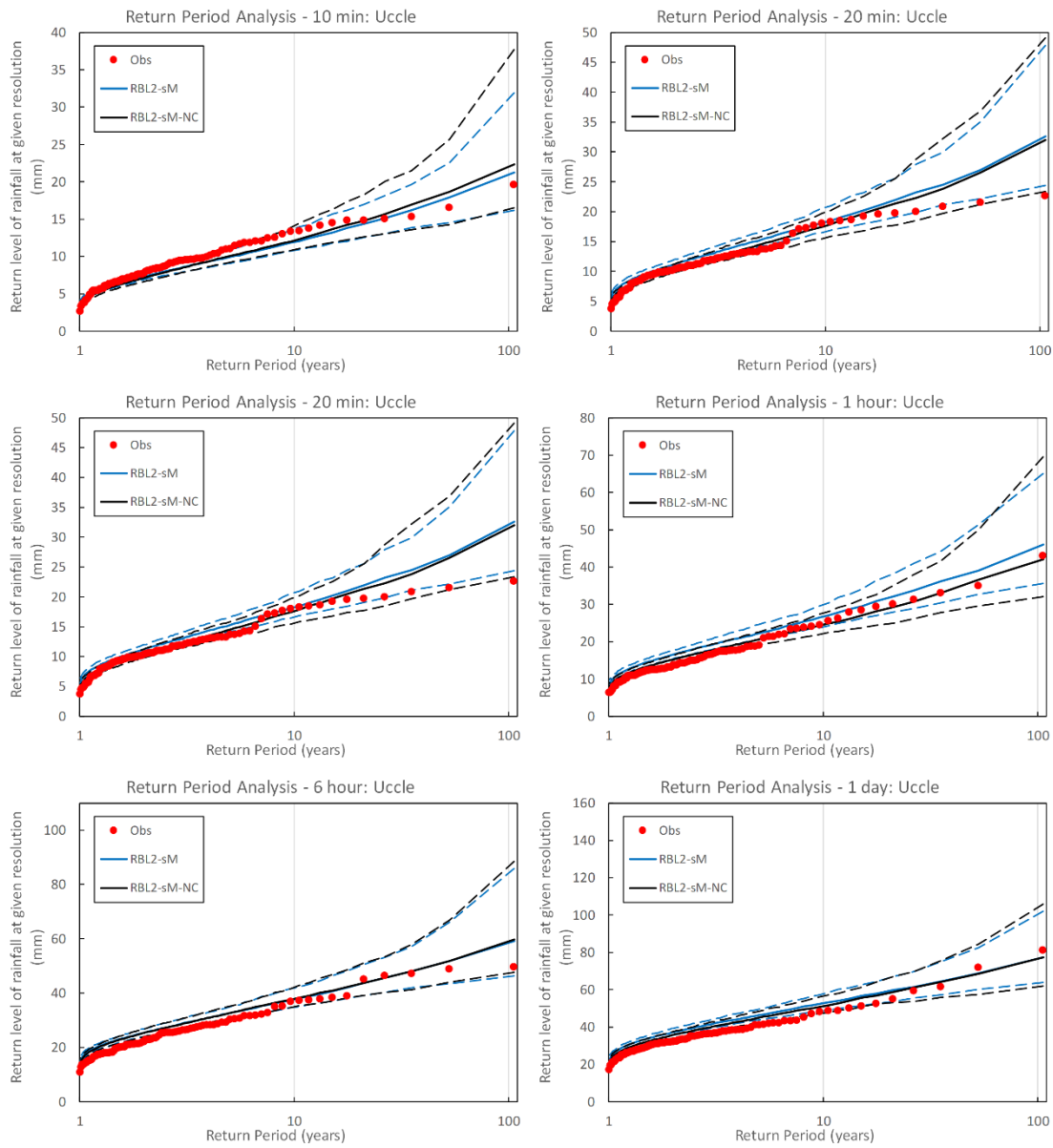


Fig. S9: Observed (round markers) and simulated (lines) return levels of rainfall at multiple time-scales at Uccle. The simulated is sampled from the RBL2 models fitted with the original (blue lines) and the new (black lines) solution spaces of α . The median and the 95- and 5-percentile return levels obtained from 250 simulations, each of 105 years, are plotted with solid and dashed lines, respectively.

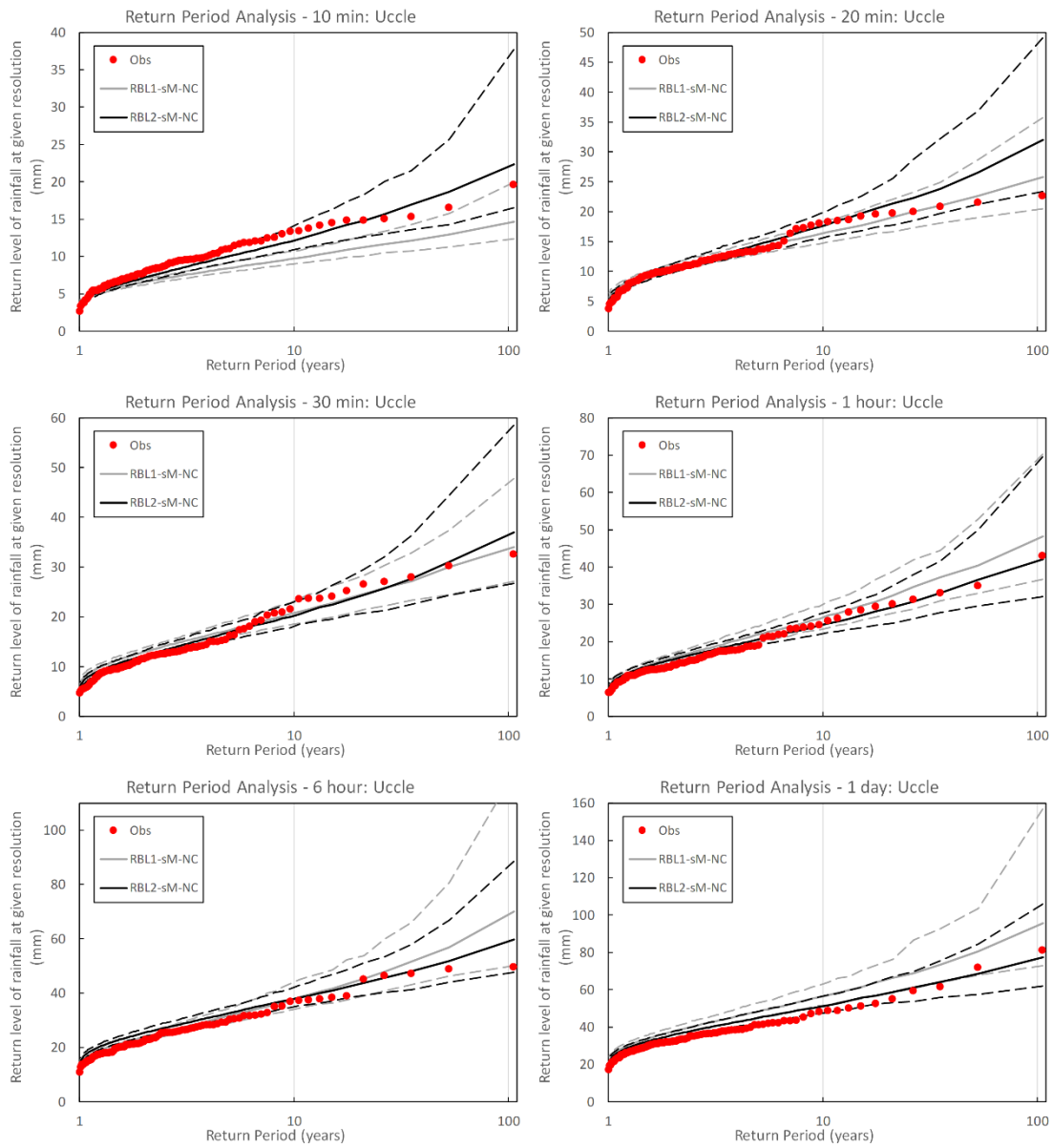


Fig. S10: Observed (round markers) and simulated (lines) return levels of rainfall at multiple time-scales at Uccle. The simulated is sampled from the RBL1 (grey lines) and RBL2 (black lines) models fitted with the new solution spaces of α . The median and the 95- and 5-percentile return levels obtained from 250 simulations, each of 105 years, are plotted with solid and dashed lines, respectively.

S4.3 Coarse-scale variances

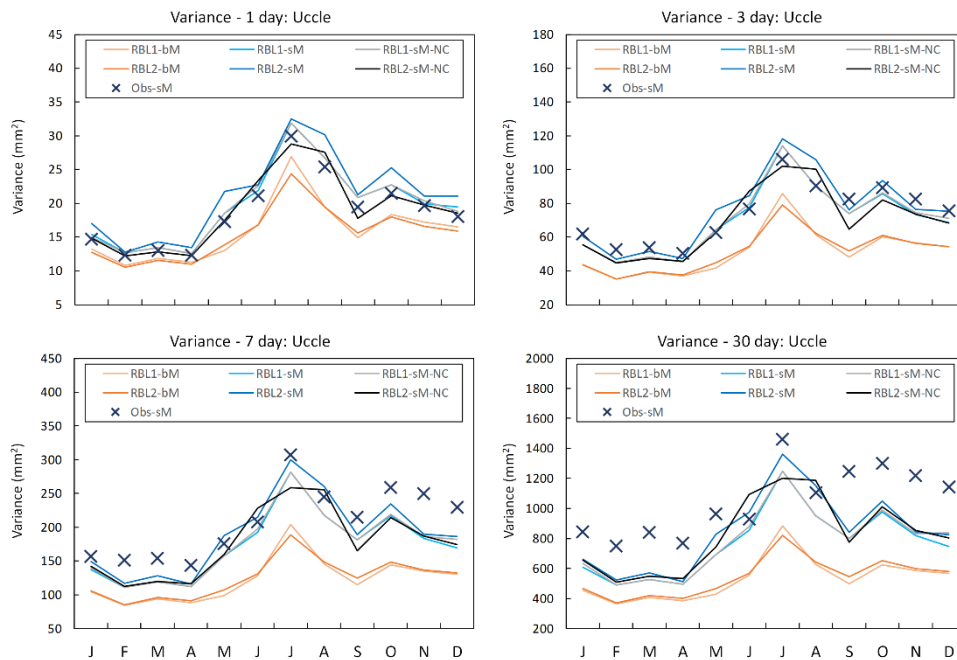


Fig. S11: Daily Variances by month at Uccle: the observed calculated with standard (Obs-sM, blue cross markers) methods, the fitted with RBL1 (RBL1-bM, light orange line; RBL1-sM, light blue line; RBL1-sM-NC, grey line) models, and the fitted with RBL2 (RBL2-bM, orange lines; RBL2-sM, blue lines; RBL2-sM-NC, black line) models.

References

Onof, C. and Wheater, H. S.: Modelling of British rainfall using a random parameter Bartlett-Lewis Rectangular Pulse Model, *Journal of Hydrology*, 149, 67 – 95, [https://doi.org/10.1016/0022-1694\(93\)90100-N](https://doi.org/10.1016/0022-1694(93)90100-N), <http://www.sciencedirect.com/science/article/pii/002216949390100N>, 1993.

Rodriguez-Iturbe, I., Cox, D. R., and Isham, V.: A point process model for rainfall: further developments, *Proceedings of the Royal Society of London A: Mathematical, Physical and Engineering Sciences*, 417, 283–298, <https://doi.org/10.1098/rspa.1988.0061>, <http://rspa.royalsocietypublishing.org/content/417/1853/283>, 1988

Wheater, H.S., Isham, V.S., Chandler, R.E., Onof, C.J., Stewart, E.J. (2006) Improved methods for national spatial-temporal rainfall and evaporation modelling for BSM. Defra, 400pp. (CEH Project no: C02056, R&D Technical Report: FD2105/TR)